

Sparse and Structured Visual Attention

Pedro Henrique Martins[‡], Vlad Niculae[‡], Zita Marinho[‡][‡], André F.T. Martins[‡][‡]

[‡]Instituto de Telecomunicações [‡]Priberam Labs [‡]Institute of Systems and Robotics [‡]Unbabel
pedrohenriqueamartins@gmail.com, vlad@vene.ro,
zita.marinho@priberam.pt, andre.martins@unbabel.com.

Abstract

Visual attention mechanisms are widely used in multimodal tasks, such as image captioning and visual question answering (VQA). One drawback of softmax-based attention mechanisms is that they assign probability mass to all image regions, regardless of their adjacency structure and of their relevance to the text. In this paper, to better link the image structure with the text, we replace the traditional softmax attention mechanism with two alternative sparsity-promoting transformations: sparsemax, which is able to select the relevant regions only (assigning zero weight to the rest), and a newly proposed Total-Variation Sparse Attention (TVMAX), which further encourages the joint selection of adjacent spatial locations. Experiments in image captioning and VQA, using both LSTM and Transformer architectures, show gains in terms of human-rated caption quality, attention relevance, and VQA accuracy, with improved interpretability.

1 Introduction

Image captioning and visual question answering (VQA) require combining natural language processing with the detection and identification of objects in an image (Farhadi et al., 2010; Kulkarni et al., 2011; Malinowski & Fritz, 2014; Xu & Saenko, 2016). While strong baselines can be achieved with general purpose encoder-decoders (Bahdanau et al., 2015; Vaswani et al., 2017), the need to link the language and vision components demands models that can incorporate structural bias. How to encourage models to look at the relevant objects only, avoiding distractions, when generating a caption or answering a question?

The current state of the art for these tasks is based on deep neural networks with visual attention (Liu et al., 2018a,b; Anderson et al., 2018; Lu et al., 2018; Kim et al., 2018; Yu et al., 2018, 2019; Tan & Bansal, 2019). These models use attention mechanisms to select either features generated by convolutional neural networks (CNNs) pretrained on image recognition datasets (He et al., 2016), or CNN features of bounding boxes (Ren et al., 2015). Bounding boxes have the advantage that the attention mechanism can attend to full objects; however, they require an external object segmentation model, that needs to be trained on a dataset annotated with groundtruth bounding boxes, which in general is very laborious to obtain. Attempts to reduce annotation efforts with unsupervised and semi-supervised techniques have considerably lower accuracy (Tao et al., 2018; Diba et al., 2019). In this paper, we focus on the former category: **visual attention** over features generated by a CNN. Without explicit object detection, the attention mechanism has to identify the relevant image regions, without object labels.

A key component of attention mechanisms is the transformation that maps scores into probabilities, with softmax being the standard choice (Bahdanau et al., 2015). However, softmax is **strictly dense**, i.e., it devotes some attention probability mass to *every* region in the image. For complex images with many objects, this may lead to “lack of focus”, originating vague captions with substantial repetitions. Figure 1 presents an example in which this is visible: in the caption generated using softmax (top), the model attends to the whole image at every step, leading to a repetition of “*bowl of fruit.*” In VQA, as shown in Figure 2, the model using softmax attends to the entire image and wrongly predicts the existence of two animals. This undesirable behavior is mitigated by using our alternative solutions: sparsemax (middle) and the newly proposed TVMAX (bottom).

In this work, we introduce novel selective visual attention mechanisms by endowing them with a new capability: that of **selecting only the relevant features of the image**. To this end, we first propose replacing softmax with **sparsemax** (Martins & Astudillo, 2016). With sparsemax, the attention weights obtained are sparse, leading to the selection (non-zero attention) of only a few relevant features. While sparsemax has been applied successfully in

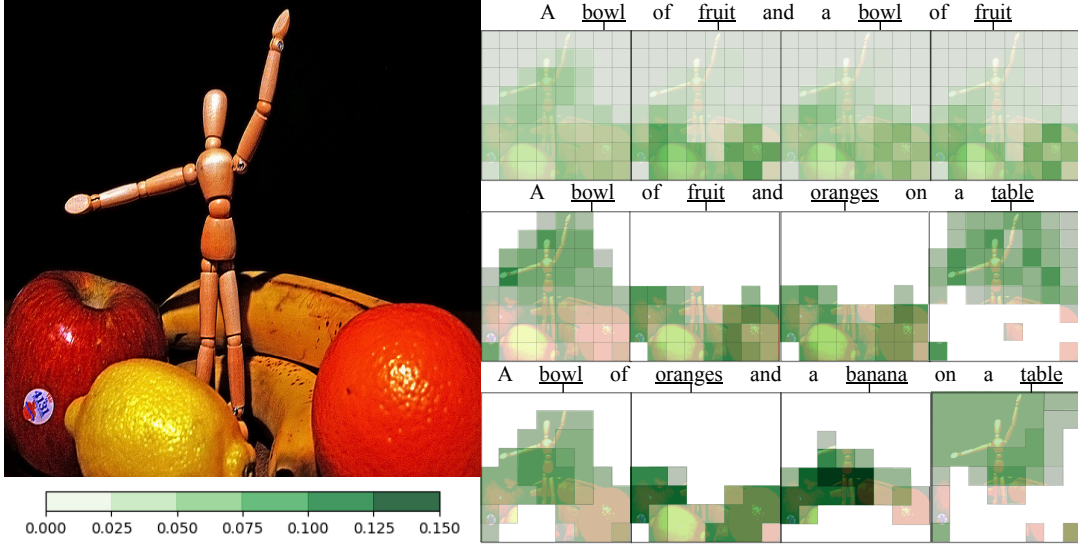


Figure 1: Captions generated using softmax (top), sparsemax (middle) and TVMAX attention (bottom). Shading denotes the attention weight, with white for zero attention. The full sequences are presented in App. B.

NLP to attend over *words*, its application to computer vision to attend over *image regions* is so far unexplored. Its effectiveness in visual domains is a hypothesis that we test in this paper. Sparsemax can also be used to select only the bounding boxes that contain relevant objects, and we show that it improves VQA accuracy while attending to only 36% of the boxes.

Second, to further encourage the weights of related adjacent spatial locations to be the same (*e.g.*, parts of an object), we introduce a new attention mechanism: **Total-Variation Sparse Attention** (which we dub TVMAX), inspired by prior work in **structured sparsity** (Tibshirani et al., 2005; Bach et al., 2012). With TVMAX, sparsity is allied to the ability of selecting *compact* regions. This leads to better interpretability, since the model’s behavior is better understood by looking at the selected image regions when a particular word is generated. It also leads to a better selection of the relevant features, and consequently to the improvement of the generated captions and to higher VQA accuracy. These improvements are corroborated in our human evaluation experiments.

To sum up, this paper introduces three main contributions:

- We propose a visual sparse attention mechanism based on sparsemax (Martins & Astudillo, 2016), which is able to *select* image regions.
- We introduce a novel attention mechanism, TVMAX, that encourages structured and sparse attention over contiguous regions, frequently parts of the same object. We show that TVMAX can be evaluated by composing a proximal operator with a sparsemax projection, and provide a closed-form expression for its Jacobian. This leads to an efficient implementation of its forward and backward passes.
- We perform empirical and qualitative comparisons of the various attention mechanisms on two tasks: image captioning and VQA. For image captioning, we also carry out human evaluation of the generated captions, as well as the perceived relevance of the selected regions.

2 Selective Visual Attention

Attention mechanisms (Bahdanau et al., 2015) have the ability to dynamically attend to relevant input features, such as spatial locations in an image. To permit end-to-end training with gradient backpropagation, they require a differentiable mapping from importance scores $z \in \mathbb{R}^k$ to a distribution $\mathbf{p} \in \Delta^k$, where $\Delta^k := \{\mathbf{p} \in \mathbb{R}^k \mid \sum_{i=1}^k p_i = 1, \mathbf{p} \geq \mathbf{0}\}$ denotes the probability simplex. The standard choice is the softmax transformation, defined as:

$$[\text{softmax}(z)]_i = \frac{\exp(z_i)}{\sum_j \exp(z_j)}. \quad (1)$$

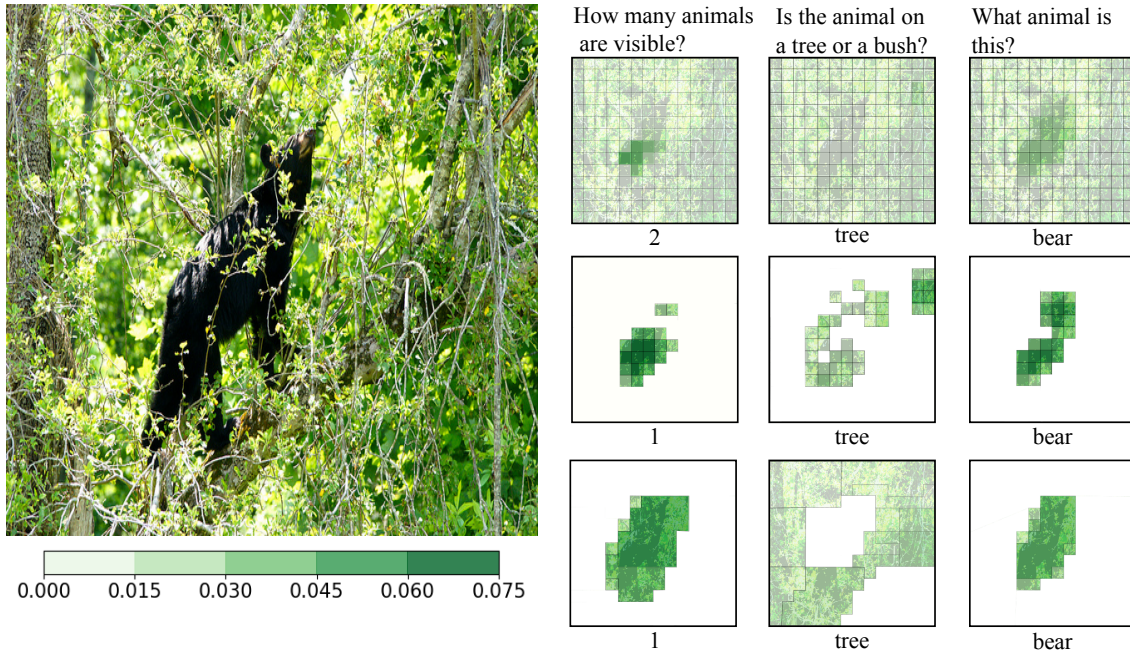


Figure 2: VQA using softmax (top), sparsemax (middle) and TVMAX attention (bottom). Shading denotes the attention weight, with white for zero attention.

Since softmax is strictly positive, its output is **dense**: it always assigns some probability mass to all image regions, even irrelevant ones. This accumulation of low probabilities may “distract” the model, preventing it from fully attending to the most relevant parts. This motivates our proposed **selective** visual attention mechanisms, which, by being sparse, are able to better isolate the relevant image regions.

2.1 Sparsemax

To achieve selective capabilities, we propose the use of **sparsemax** (Martins & Astudillo, 2016), a sparse mapping consisting in the Euclidean projection of z onto the simplex:

$$\text{sparsemax}(z) := \arg \min_{p \in \Delta^k} \frac{1}{2} \|p - z\|_2^2. \quad (2)$$

Sparsemax encourages sparse outputs, corresponding to the boundary of Δ^k . This is an attractive property for visual attention mechanisms, where often only a few features provide relevant information for the current prediction. Using sparsemax allows focusing only on relevant image locations, assigning zero attention weight to all other regions.

2.2 Sparse and Structured Visual Attention

While sparsity can be useful in visual attention, it might not be enough. To generate descriptive captions or answer specific questions, the model needs to identify the full objects present in the image, i.e., the selected regions should be encouraged to have a compact structure. However, sparsemax is **unstructured** and **index-invariant**, leading it to select discontinuous regions. To overcome this, we propose a new visual attention mechanism, **TVMAX**. TVMAX is a (non-trivial) generalization of fusedmax (Niculae & Blondel, 2017), a transformation based on fused lasso, to the 2D case. For ease of exposition, we first describe how fused lasso is extended to arbitrary graphs, and then we particularize to the 2D case.

2.2.1 Generalized Fused Lasso

Let $w \in \mathbb{R}^k$ be a vector of weights, and (I, E) be an undirected graph, where $I = \{1, \dots, k\}$ and $E \subseteq I \times I$. Two nodes i and j are connected by an edge in E (denoted $i \sim j$), whenever they are encouraged to have similar

weights, $w_i \approx w_j$. The generalized fused lasso penalty (Tibshirani et al., 2005) is defined as:

$$\Omega_E(\mathbf{w}) = \sum_{(i,j) \in E} |w_i - w_j|. \quad (3)$$

Minimizing Ω_E encourages “fused” solutions, i.e., it encourages $w_i = w_j$ for $i \sim j$. In particular, its proximal operator¹ can be seen as a **fused signal approximator**, seeking a vector \mathbf{w} that approximates \mathbf{z} well (in terms of Euclidean distance) and that is encouraged to be fused:

$$\text{prox}_{\lambda\Omega_E}(\mathbf{z}) = \arg \min_{\mathbf{w} \in \mathbb{R}^d} \frac{1}{2} \|\mathbf{w} - \mathbf{z}\|_2^2 + \lambda\Omega_E(\mathbf{w}). \quad (4)$$

Computing the value of $\text{prox}_{\lambda\Omega_E}$ is non-trivial in general (Xin et al., 2016), but for certain edge configurations, described below, efficient algorithms exist.

- If E forms a chain, i.e. $i \sim j \iff i = j - 1$, the problem is called **1D total variation**, $\Omega_{1D}^{TV}(\mathbf{w}) := \sum_{i=1}^{k-1} |w_{i+1} - w_i|$. It can be solved in $\mathcal{O}(k)$ time using the *taut string algorithm* (Davies & Kovac, 2001; Barbero & Sra, 2014). We use the quasilinear algorithm of Condat (2013), which is very fast in practice.
- If the indices are aligned on a 2D grid, as in an image, the problem is called **2D total variation** and the penalty is defined as:

$$\Omega_{2D}^{TV}(\mathbf{W}) := \sum_i \Omega_{1D}^{TV}(\mathbf{w}_{i,:}) + \sum_j \Omega_{1D}^{TV}(\mathbf{w}_{:,j}), \quad (5)$$

where $\mathbf{w}_{i,:}$ and $\mathbf{w}_{:,j}$ denote the rows and columns of \mathbf{W} , respectively. Unlike the 1D case, exact algorithms are not available. However, for an input of size $a \times b$, it is possible to *split* the penalty into a column-wise and b row-wise 1D problems, and then apply iterative methods, for instance the proximal Dykstra algorithm (Barbero & Sra, 2014).²

2.2.2 TVMAX

TVMAX combines 2D total variation (TV2D) regularization with sparsemax. This way, it promotes sparsity and encourages the attention weights of adjacent spatial locations to be the same, selecting contiguous regions of the image. TVMAX is defined as follows:

Definition 1 (TVMAX). *Let $\mathbf{z} \in \mathbb{R}^k$, such that the indices of \mathbf{z} can be decomposed into rows and columns. The TVMAX transformation is defined as*

$$\text{TVMAX}(\mathbf{z}) := \arg \min_{\mathbf{p} \in \Delta^k} \frac{1}{2} \|\mathbf{p} - \mathbf{z}\|_2^2 + \lambda\Omega_{2D}^{TV}(\mathbf{p}), \quad (6)$$

where λ is an hyper-parameter controlling the amount of fusion ($\lambda = 0$ recovers sparsemax) and Ω_{2D}^{TV} is a 2D total variation penalty, defined as in Eq. 5.

Note that Eq. 6 differs from Eq. 4: the variable \mathbf{p} is further constrained to lie in the simplex. We show next how the forward and backward passes can be efficiently computed.

2.3 TVMAX’s Forward and Backward passes

We will now derive the forward and backward passes for the **generalized fused sparse attention**. We follow Niculae & Blondel (2017) and define

$$\text{gfusedmax}_E(\mathbf{z}) := \arg \min_{\mathbf{p} \in \Delta^k} \|\mathbf{p} - \mathbf{z}\|_2^2 + \lambda\Omega_E(\mathbf{p}). \quad (7)$$

This can be seen as a *constrained* fused lasso approximator, because the solution \mathbf{p} must be a probability distribution vector. While the optimization function is very similar to Eq. 4, note the additional constraint $\mathbf{p} \in \Delta^k$. Fortunately, the following result holds (see App. A.2 for a proof):

Proposition 1. *The generalized fusedmax can be expressed as*

$$\text{gfusedmax}_E(\mathbf{z}) = \text{proj}_{\Delta^k}(\text{prox}_{\lambda\Omega_E}(\mathbf{z})). \quad (8)$$

¹The proximal operator of a function $f: \mathbb{R}^d \rightarrow \mathbb{R} \cup \{\infty\}$ is defined as $\text{prox}_f(\mathbf{z}) = \arg \min_{\mathbf{w} \in \mathbb{R}^d} \frac{1}{2} \|\mathbf{w} - \mathbf{z}\|_2^2 + f(\mathbf{w})$.

²We use the implementation readily available in the `copt` library, available at <http://openopt.github.io/copt/>.

This result shows that `gfusedmax`'s forward pass can be computed simply by composing the proximal step of fused lasso with the forward pass of `sparsemax`. Proposition 1 also provides a shortcut for deriving the Jacobian of generalized fusedmax via the *chain rule*: denoting by \mathbf{J}_F the Jacobian of $\text{prox}_{\lambda\Omega_E}$, we have

$$\frac{\partial \text{gfusedmax}}{\partial \mathbf{z}} = \mathbf{J}_{\text{sparsemax}}(\text{prox}_{\lambda\Omega_E}(\mathbf{z}))\mathbf{J}_F(\mathbf{z}). \quad (9)$$

The form of $\mathbf{J}_{\text{sparsemax}}$ has been studied by Martins & Astudillo (2016) (we include it for completeness in App. A.1). The next proposition completes the puzzle, giving a full characterization of \mathbf{J}_F .

Proposition 2 (Group-wise characterization of $\text{prox}_{\lambda\Omega_E}$). *Let $\mathbf{w}^* := \text{prox}_{\lambda\Omega_E}(\mathbf{z})$, and denote by G_i the set of indices fused to w_i in the solution, G_i may be defined recursively:*

1. $i \in G_i$ for all i , and
2. $j \in G_i$ if there exists $m \in G_i$ such that $m \sim j$ and $w_m^* = w_j^*$.

Define $s_{ij} = \text{sign}(w_i^* - w_j^*)$. Then, we have

$$w_i^* = \frac{1}{|G_i|} \sum_{j \in G_i} \left(z_j + \sum_{\substack{m \sim j \\ m \notin G_i}} \lambda s_{mj} - \sum_{\substack{j \sim m \\ m \notin G_i}} \lambda s_{jm} \right). \quad (10)$$

Proposition 2 shows how to easily compute a generalized Jacobian of `gfusedmax`: since small perturbations in \mathbf{z} never change the groups G_i nor the signs of across-group differences s_{ij} , differentiating Eq. 10 yields

$$(\mathbf{J}_F)_{i,j} = \frac{\partial w_i^*}{\partial z_j} = \begin{cases} \frac{1}{|G_i|}, & j \in G_i, \\ 0, & j \notin G_i. \end{cases} \quad (11)$$

This generalizes Lemma 1 of Niculae & Blondel (2017) to arbitrary graphs, with a simpler proof, in App. A.3.

2.3.1 COMPUTATION

As we show in Proposition 1, computing `TVMAX`'s forward pass can be done by chaining efficient algorithms for `TV2D` and `sparsemax`.

From Eq. 9 we have that `TVMAX`'s Jacobian can be computed by composing the Jacobian of the Total Variation proximal operator, \mathbf{J}_F , and $\mathbf{J}_{\text{sparsemax}}$, which is known. As derived in Proposition 2, $(\mathbf{J}_F)_{i,j} = 1/n_{ij}$ if i and j are fused in a group with n_{ij} elements, and 0 otherwise. Thus, the backward pass intuitively involves "spreading" the credit assigned to one image location evenly across all locations fused with it. This can be implemented by Algorithm 1 in $\mathcal{O}(N_g \log k)$ where N_g is the number of groups of fused positions. In the worst case, when there are no positions fused, the complexity is $\mathcal{O}(k \log k)$. This algorithm is inspired by flood filling algorithms (Burtsev & Kuzmin, 1993).

3 Experiments

We compare our proposed visual attention mechanisms on two tasks: image captioning (§3.1) and VQA (§3.2). In image captioning the goal is to generate a textual description for a given image, while in VQA the goal is to answer a natural language question about the image. Our experiments encompass three different architectures: LSTM and Transformer with ResNet features as input, and Transformer with bounding box features as input.

3.1 Image Captioning

For image captioning, we use as the underlying architecture an LSTM encoder-decoder model with visual attention, inspired by Liu et al. (2018a). Given an image, we use a residual CNN, ResNet, pretrained on ImageNet (He et al., 2016; Russakovsky et al., 2014) to get a feature map with spatial dimension of size 8×8 and channel dimension of size 2048, that go through a feedforward layer yielding $g = 512$ feature maps. The visual feature matrix $\mathbf{V} = [v_1, v_2, \dots, v_k]$, with $v_i \in \mathbb{R}^g$ and $k = 64 = 8 \times 8$, contains the image information. Following Liu et al. (2018a), we use input and output attention to select the relevant features for the current generation. To

Algorithm 1 TVMAX backward pass

```

1 Input:  $\mathbf{p} = \text{TVMAX}(\mathbf{z}), \mathbf{dp} \in \mathbb{R}^k$ .
2 Output:  $\mathbf{dz} = \mathbf{J}_{\text{TVMAX}}^\top(\mathbf{dp}) \in \mathbb{R}^k$  # chain rule
3 Initialize:  $N \leftarrow \emptyset$  # neighbours stack
4  $V \leftarrow \emptyset$  # visited positions
5  $G \leftarrow \emptyset$  # current group
6  $s = 0$  # intermediate value used for  $J_{\text{TVMAX}}$ 's computation
7  $\mathbf{dw} \leftarrow (\mathbf{J}^{\text{sp}})^\top \mathbf{dp}$  # Eqs. 15 and 16 of §A.1
8 while  $|V| < k$  do # check if all positions have been visited
9   pick  $(i_0, j_0) \notin V$ , push  $(i_0, j_0)$  to  $N$  # get not visited position and add it to neighbours stack
10  while  $N$  not empty do
11    pop  $(i, j)$  from  $N$  # get element from neighbours stack
12    if  $p_{i,j} = p_{i_0,j_0}$  then # check if element is fused
13       $G \leftarrow G \cup \{(i, j)\}, V \leftarrow V \cup \{(i, j)\}$  # add neighbour to group and to visited positions
14       $s \leftarrow s + (\mathbf{dw})_{i,j}$  # sum of the  $\mathbf{dw}$  of each element of the group
15      for all neighbours  $(i', j') \sim (i, j)$  do
16        if  $(i', j') \notin V$  then push  $(i', j')$  to  $N$  # add not visited neighbours of  $(i, j)$  to the stack
17    if  $G$  not empty then:
18       $(\mathbf{dz})_{i,j} \leftarrow s/|G|$  for all  $(i, j) \in G$  # compute  $J_{\text{TVMAX}}$  for elements in group  $G$ 
19       $G \leftarrow \emptyset$ 
20       $s = 0$ 

```

Table 1: Automatic evaluation of caption generation on MSCOCO and Flickr30k.

	MSCOCO						Flickr30k					
	SPICE	CIDER	ROUGE _L	BLEU ₄	METEOR	REP↓	SPICE	CIDER	ROUGE _L	BLEU ₄	METEOR	REP↓
softmax	18.4	0.967	52.9	29.9	24.9	3.76	13.5	0.443	44.2	19.9	19.1	6.09
sparsemax	18.9	0.990	53.5	31.5	25.3	3.69	13.7	0.444	44.3	20.7	19.3	5.84
TVMAX	18.5	0.974	53.1	29.9	25.1	3.17	13.3	0.438	44.2	20.5	19.0	3.97

generate the word at position t , the **input attention**, α_t , is computed using the LSTM’s previous hidden state, $\mathbf{h}_{t-1} \in \mathbb{R}^d$. First, an importance score $z_{t,i}, i \in \{1, \dots, k\}$, is computed between \mathbf{h}_{t-1} and the i^{th} image cell via a feedforward transformation (Bahdanau et al., 2015), as $z_{t,i} = \mathbf{w}^\top \tanh(\text{affine}([v_i; \mathbf{h}_{t-1}]))$, for all k image cells. Then, α_t is obtained by normalizing the k -dimensional vector of scores \mathbf{z}_t with softmax, $\alpha_t = \text{softmax}(\mathbf{z}_t)$. Using these attention weights, a vector representation of the image to be used as input of the LSTM, is obtained, $\mathbf{s}_t = \mathbf{V}\alpha_t$. The **output attention** $\tilde{\alpha}_t$, used to select the relevant visual features to generate the current word, is computed in the same way, but applied to the current LSTM hidden state \mathbf{h}_t , instead of \mathbf{h}_{t-1} , and normalized with the different proposed transformations. This produces output visual features $\tilde{\mathbf{s}}_t = \mathbf{V}\tilde{\alpha}_t$, which are passed through a feedforward layer to yield the image representation $\mathbf{r}_t = \tanh(\text{affine}(\tilde{\mathbf{s}}_t))$. Finally, the predictive probability of the next word is $P(y_t | y_{1:(t-1)}; V) \propto \text{softmax}(\text{affine}([\mathbf{r}_t; \mathbf{h}_t]))$.

Settings. The input images are resized to 256×256 before going through the ResNet. We use an LSTM hidden size of 512 and a word embedding size of 256. The models were trained for 50 epochs using the Adam optimizer (Kingma & Ba, 2014) with a learning rate of 0.0001 and a decay of 0.8 and 0.999 for the first and second momentum. After the 10^{th} epoch, the learning rate starts decaying with a decay factor of 0.99, every epoch. For TVMAX, we set $\lambda = 0.01$.

Datasets and metrics. We report results on the Microsoft COCO (MSCOCO) and Flickr30k datasets (Lin et al., 2014; Young et al., 2014). MSCOCO is composed of 113,287 images of common objects in context while Flickr30k consists of 31,000 pictures of people in everyday activities. Each image is annotated with 5 captions. We use the split proposed by Karpathy & Fei-Fei (2015), which stipulates equal validation and test sizes of 5,000 images (MSCOCO) and 1,000 (Flickr30k). The metrics we report are SPICE (Anderson et al., 2016), CIDEr (Vedantam et al., 2015), longest common subsequence ROUGE, (denoted ROUGE_L; Lin, 2004), 1– to 4–gram BLEU (denoted BLEU₄; Papineni et al., 2002), and METEOR (Banerjee & Lavie, 2005). To investigate if selective attention alleviates repetition, we also measure the n-gram repetition metric REP (Malaviya et al., 2018).

Automatic metrics. State-of-the-art results are reported by Wang et al. (2019): SPICE and CIDEr scores of 21.5 and 121.7 by attending to semantic concepts, bounding box, and ResNet features. Since our focus is to compare different visual attention mechanisms, we opted for a simpler, less engineered, model to compare the proposed transformations, attending only to ResNet features; this way we filter out effects that could be caused by other system’s components. As can be seen in Table 1, sparsemax and TVMAX achieve better results overall when compared with softmax, indicating that the use of selective attention leads to better captions. This improvement does not come at a high computational cost: at inference time, models using TVMAX and sparsemax are only 1.3x and 1.1x slower than softmax. Moreover, for TVMAX, automatic metrics results are slightly worse than sparsemax but still superior to softmax on MSCOCO and similar on Flickr30k. We show next that this is compensated with fewer repetitions and higher scores in the human evaluation of the captions and attention relevance.

Human rating. We conducted a human evaluation study to assess the captions quality and the attention relevance. The caption evaluation consisted in attributing a score (1 to 5) to the caption of each model, while the attention evaluation consisted in scoring (1 to 5) the relevance of the attended areas when generating the caption words (excluding stop-words). A full description can be found in App. C.

Table 2: Human evaluation results on MSCOCO.

	CAPTION	ATTENTION RELEVANCE
softmax	3.50	3.38
sparsemax	3.71	3.89
TVMAX	3.87	4.10

Despite performing slightly worse than sparsemax under automatic metrics, TVMAX outperforms sparsemax and softmax in the caption human evaluation and the attention relevance human evaluation, reported in Table 2. The superior score on attention relevance shows that TVMAX is better at selecting the relevant features and its output is more interpretable. Additionally, the better caption evaluation results demonstrate that the ability to select compact regions induces the generation of better captions. We next explore possible explanations for the TVMAX superior results.

Repetition. Figure 1 illustrates that softmax attention is prone to spuriously repeating references to the same object. Selective attention mechanisms like sparsemax and especially TVMAX reduce repetition, as measured by the REP metric reported in Table 1. This expected success can be attributed to the sparsity of the attention weights distribution and to the ability to select compact regions exclusively and can be one of the causes of the human evaluation results. This happens even though TVMAX generates longer sentences than sparsemax and softmax (9.5 against 9.0 words on average) and shows the benefit of promoting structured and sparse attention simultaneously. To corroborate our intuition that sparsity leads to less repetition, we measured the Jensen-Shannon divergence (JS) between the attention distributions for each step of the generation of the captions correspondent to the images of the MSCOCO test set. The mean JS values are 0.12, 0.29, and 0.34 for softmax, sparsemax, and TVmax, respectively. This shows that sparsity leads to less similar attention distributions along the generation of the captions and, consequently, to less repetitions.

Object detection. Using the MSCOCO object detection groundtruth, we compared the percentage of objects present in the image that are referred to in the captions, using each attention mechanism. With TVMAX 28.2% of the reference objects are referred, against 27.5% and 27.4% for sparsemax and softmax, respectively. This shows that promoting high attention to groups of spatial locations of the image leads to a more precise identification of the objects.

Sparsity. The mean image area that receives zero attention is 34% for sparsemax and 25% for TVMAX. As can be seen Figure 1, as expected, softmax weights are spread widely across the image, ending up missing the relevant regions. In contrast, sparsemax and TVMAX weights are zero for the non-relevant spatial locations.

Qualitative comparison. As the image of Figure 1 contains various similar objects, the softmax model generates a incoherent, repetition-laden caption. In contrast, the sparsemax and TVMAX models better identify the relevant parts of the image, generating coherent and descriptive captions. Moreover, the groups obtained with TVMAX are clearly visible and more aligned to object boundaries, offering better interpretability, as revealed by human attention assessment.

3.2 Visual Question Answering

Table 3: Automatic evaluation of VQA on VQA-2.0. Sparse-TVMAX and soft-TVMAX correspond to using sparsemax or softmax on the image self-attention and TVMAX on the output attention. Other models use softmax or sparsemax on self-attention and output attention.

		Att. to image	Att. to bounding boxes	Test-Dev			Test-Standard				
				Yes/No	Number	Other	Overall	Yes/No	Number	Other	Overall
softmax	✓			83.08	42.65	55.74	65.52	83.55	42.68	56.01	65.97
sparsemax	✓			83.08	43.19	55.79	65.60	83.33	42.99	56.06	65.94
soft-TVMAX	✓			<u>83.13</u>	<u>43.53</u>	56.01	65.76	83.63	<u>43.24</u>	56.10	66.11
sparse-TVMAX	✓			83.10	43.30	<u>56.14</u>	<u>65.79</u>	<u>83.66</u>	43.18	<u>56.21</u>	<u>66.17</u>
softmax			✓	85.14	49.59	<u>58.72</u>	68.57	85.56	49.54	<u>59.11</u>	69.04
sparsemax			✓	85.40	50.87	58.67	<u>68.79</u>	85.80	<u>50.18</u>	59.08	<u>69.19</u>
softmax	✓		✓	85.33	50.49	58.88	68.82	85.58	50.42	59.18	69.17
sparse-TVMAX	✓		✓	<u>85.35</u>	<u>50.52</u>	59.15	68.96	<u>85.72</u>	50.66	59.22	69.28

To compare the attention mechanisms in VQA, we perform experiments with the encoder-decoder version of deep Modular Co-Attention Networks (MCAN; Yu et al., 2019). When performing VQA, we are given an input image and a question about it. To represent the question’s words we use 300-dimensional GloVe word embeddings (Pennington et al., 2014). To represent the image we use a ResNet pretrained on ImageNet (He et al., 2016; Russakovsky et al., 2014) (“Att. to image” in Table 3). The CNN outputs a feature map with spatial dimension of size $N = 14 \times 14$ and channel dimension of size 2048, that goes through a feed-forward layer yielding 512 feature maps. The encoder, used to learn the question representation, consists of a Transformer-like architecture (Vaswani et al., 2017), whose input is the embedding representation of the words in the question and its output the representation of the question, \mathbf{X} . The decoder, used to learn the image representation, is similar to the encoder but has additional guided-attention layers in which the question representation \mathbf{X} is used to guide the attention given to the image features. The inputs of the decoder are the image feature maps and its output corresponds to the image representation, \mathbf{Y} . To obtain the final question and image representations, $\tilde{\mathbf{x}}$ and $\tilde{\mathbf{y}}$, an output attention layer is used to attend over the representations \mathbf{X} and another to attend over \mathbf{Y} as $\tilde{\mathbf{y}} = \sum_{i=1}^N \alpha_i \mathbf{y}_i$, where $\alpha = \rho(\text{affine}(\mathbf{Y}))$, where the transformation ρ is either softmax, sparsemax, or TVMAX for the image representation, and softmax for the question representation. This is followed by pooling: $\mathbf{z} = \text{LayerNorm}(\mathbf{W}_x \tilde{\mathbf{x}} + \mathbf{W}_y \tilde{\mathbf{y}})$. Finally, the predicted answer to the question is obtained by projecting \mathbf{z} into a vector $\mathbf{s} \in \mathbb{R}^N$ followed by a sigmoid function, where N is the number of possible answers.

Additionally, to observe the benefits of attending only to the relevant bounding boxes, we experiment using sparsemax to attend to bounding box features extracted with Faster R-CNN (Ren et al., 2015) pretrained on Visual Genome (Krishna et al., 2017) (“Att. to bounding boxes” in Table 3). The only difference in the architecture is the use of bounding box features as input, instead of ResNet features. Thus, we have $\mathbf{z} = \text{LayerNorm}(\mathbf{W}_x \tilde{\mathbf{x}} + \mathbf{W}_b \tilde{\mathbf{y}}_b)$, where $\tilde{\mathbf{y}}_b$ is the final image representation when we use bounding box features.

To understand whether ResNet features can be used as a complement to bounding box features, we combine two decoders, having one the ResNet features as input and the other bounding box features. The image representations obtained by the decoders are then combined with the question representation, $\mathbf{z} = \text{LayerNorm}(\mathbf{W}_x \tilde{\mathbf{x}} + \mathbf{W}_y \tilde{\mathbf{y}} + \mathbf{W}_b \tilde{\mathbf{y}}_b)$.

Settings. The input images are resized to 448×448 before going through the ResNet. We use a model with 6 layers of multi-head attention with 8 heads. The models were trained for 15 epochs using the Adam optimizer (Kingma & Ba, 2014) with a learning rate of $\min(2.5t \cdot 10^{-5}, 1 \cdot 10^{-4})$, where t is the epoch number starting from 1. After 10 epochs, the learning rate is multiplied by $1/5$ every 2 epochs. We set $\lambda = 0.01$ for TVMAX. Note that the models were trained only on the train set, without data augmentation.

Datasets and metrics. We report the results on the widely used VQA-v2 dataset (Goyal et al., 2017). It is composed of the MSCOCO images, annotated with several questions per image and 10 answers per question. The train set is composed of 82,783 images and 443,757 questions while the validation and test sets have 40,504 images and 214,354 questions, and 81,434 images and 447,793 questions, respectively. The test set is subdivided into 4

splits: test-dev, test-standard, test-challenge and test-reserve. We report results in the test-dev and test-standard.³ The results reported correspond to the per-type (Yes/No, Number, and Other) accuracies and the overall accuracy.

Results. State-of-the-art results are reported by Yu et al. (2019), accuracy of 70.90 on the test-standard, by training on the train and validation splits, and visual genome, and Tan & Bansal (2019), accuracy of 72.50 on test-standard, by performing pretraining on a big dataset. In this paper, we do not perform any data augmentation, training only on the train set, and achieve results on par with state-of-the-art models trained with the same data (Yu et al. (2018) report an accuracy of 65.80 with a single model and of 68.02 with an ensemble of 6 models, on the test-dev). Their contributions are orthogonal and can be combined with ours.

As can be seen in the results presented in Table 3 the models using TVMAX in the output attention layer outperform the models using softmax and sparsemax. Moreover, the results are slightly superior when the sparsemax transformation is used in the self-attention layers of the decoder. It can also be observed that, when using sparsemax both in the self-attention layers of the decoder and in the output attention mechanism, the accuracy is superior than when using softmax. Thus, having sparse attention mechanisms in the self-attention layers is beneficial, but the biggest improvement is obtained when using TVMAX in the output attention. This corroborates our intuition that selecting the features of contiguous regions of the image leads to a better understanding of the image, and, consequently, better accuracy. Additionally, when using bounding box features, sparsemax outperforms softmax, showing that selecting only the bounding boxes of the relevant objects leads to a better answering capability. We can also see that combining ResNet features with bounding box features improves results. Moreover, the model using TVMAX in the final attention layer achieves the highest accuracy, showing that features obtained using the TVMAX transformation are a better complement to bounding box features.

Sparsity. For the models using ResNet features, the mean image area that have attention weight of 0, on the final attention layer, is 68% when using sparsemax and 58% when using TVMAX. When using sparsemax over bounding boxes, 64% of the bounding boxes receive an attention weight of 0, only 12 bounding boxes being selected on average.

Qualitative comparison. Figure 2 illustrates an example using the different attention mechanisms. We can see that the softmax model, by attending to the whole image, wrongly predicts the existence of two animals. This is mitigated by sparsemax and TVMAX. Moreover, we can clearly see the groups of regions obtained with TVMAX, which are closely aligned with the boundaries of the objects. This is a common behavior that is also present in Figure 5 of App. B.

4 Related Work

Sparse attention. In several tasks only a few features are relevant for the current prediction. This can be attained when using sparse attention. Various prior works have proposed sparse attention mechanisms with promising results, (Xu et al., 2015; Martins & Astudillo, 2016; Malaviya et al., 2018; Peters et al., 2019). Niculae & Blondel (2017) proposed 1D fusedmax, which incorporates the fused lasso, so that adjacent words are encouraged to have the same attention weight. In this work, the authors were able to improve interpretability, obtaining superior results on textual entailment and summarization. We derive a generalized fused attention mechanism, extending 1D fusedmax.

Image captioning. Neural models with visual attention mechanisms have been receiving increased interest. Researchers have been studying diverse attention mechanisms to refine visual information for image captioning. Xu et al. (2015) proposed hard attention, which only attends to one region at each step. However, to generate descriptive captions the model should, often, focus on more than one region. In addition, hard attention is non-differentiable, requiring imitation learning or Monte Carlo policy gradient approximations. Anderson et al. (2018) proposed attending to bounding box features detected by an object detection model. Gao et al. (2019) introduced a deliberate attention network. Wang et al. (2019) proposed an hierarchical attention network composed by a patch detector, object detector, and concept detector. Our work is orthogonal and can be combined with the models depicted.

Visual question answering. Similarly to image captioning, neural models with visual attention are the state-of-the-art in VQA. Networks with attention layers are used to obtain a representation of the question and image, which are then fused to predict the answer. Several works focused on methods for fusing the image and question representations (Fukui et al., 2016; Ben-Younes et al., 2017; Kim et al., 2017; Yu et al., 2017, 2018). Another line

³Models evaluated on <https://evalai.cloudcv.org/web/challenges/challenge-page/163/overview>.

of work focus on improving the visual attention, which is performed over the image grid obtained with a pretrained CNN or over bounding boxes (Anderson et al., 2018). Yang et al. (2016) proposed a stacked attention network over the image to learn the features iteratively. Lu et al. (2016) introduced a hierarchical co-attention model and Nam et al. (2017) proposed using a multi-stage co-attention model. Recently, Yu et al. (2019) introduced a co-attention Transformer-like model and Tan & Bansal (2019) proposed pretraining a Transformer on an aggregated dataset to improve the model’s initialization. Our proposed attention mechanisms can be combined with the models described.

5 Conclusions and Future Work

We propose using sparse and structured visual attention to improve the process of selecting the relevant features. For that, we used sparsemax and introduced TVMAX. Results on image captioning and VQA show that the attention mechanism is able to select better features when using sparsemax or TVMAX. Furthermore, in the image captioning human assessment and attention analysis we see that the improved selection of the relevant features as well as the ability to group spatial features lead to the generation of better captions, while improving the model’s interpretability.

In future work, fused sparse attention can be applied in other tasks for which we have prior knowledge of the data’s structure, for instance graphs or trees.

Acknowledgements

This work was supported by the European Research Council (ERC StG DeepSPIN 758969), and by the Fundação para a Ciência e Tecnologia through contracts UID/EEA/50008/2019 and CMUPERI/TIC/0046/2014 (GoLocal). We thank Jack Hessel, David Vicente, Gonçalo Correia, Erick Fonseca, Marcos Treviso, and Tsvetomila Mihaylova for helpful discussion and feedback.

References

- Anderson, P., Fernando, B., Johnson, M., and Gould, S. SPICE: Semantic propositional image caption evaluation. In *Proc. ECCV*, 2016.
- Anderson, P., He, X., Buehler, C., Teney, D., Johnson, M., Gould, S., and Zhang, L. Bottom-Up and Top-Down Attention for Image Captioning and Visual Question Answering. In *Proc. CVPR*, 2018.
- Bach, F., Jenatton, R., Mairal, J., Obozinski, G., et al. Optimization with sparsity-inducing penalties. *Foundations and Trends in Machine Learning*, 2012.
- Bahdanau, D., Cho, K., and Bengio, Y. Neural machine translation by jointly learning to align and translate. In *Proc. ICLR*, 2015.
- Banerjee, S. and Lavie, A. METEOR: An automatic metric for MT evaluation with improved correlation with human judgments. In *Proc. ACL Workshop on Intrinsic and Extrinsic Evaluation Measures for Machine Translation and/or Summarization*, 2005.
- Barbero, A. and Sra, S. Modular proximal optimization for multidimensional total-variation regularization. *preprint arXiv:1411.0589*, 2014.
- Ben-Younes, H., Cadene, R., Cord, M., and Thome, N. Mutan: Multimodal tucker fusion for visual question answering. In *Proc. ICCV*, 2017.
- Burtsev, S. and Kuzmin, Y. An efficient flood-filling algorithm. *Computers & Graphics*, 1993.
- Condat, L. A direct algorithm for 1-d total variation denoising. *IEEE Signal Processing Letters*, 20(11):1054–1057, 2013.
- Davies, P. L. and Kovac, A. Local extremes, runs, strings and multiresolution. *The Annals of Statistics*, 2001. ISSN 00905364.
- Diba, A., Sharma, V., Stiefelhagen, R., and Van Gool, L. Weakly Supervised Object Discovery by Generative Adversarial & Ranking Networks. In *Proc. CVPR Workshops*, 2019.

- Farhadi, A., Hejrati, M., Sadeghi, M. A., Young, P., Rashtchian, C., Hockenmaier, J., and Forsyth, D. Every picture tells a story: Generating sentences from images. In *Proc. ECCV*, 2010.
- Friedman, J., Hastie, T., Höfling, H., and Tibshirani, R. Pathwise coordinate optimization. *The Annals of Applied Statistics*.
- Fukui, A., Park, D. H., Yang, D., Rohrbach, A., Darrell, T., and Rohrbach, M. Multimodal Compact Bilinear Pooling for Visual Question Answering and Visual Grounding. In *Proc. EMNLP*, 2016.
- Gao, L., Fan, K., Song, J., Liu, X., Xu, X., and Shen, H. T. Deliberate Attention Networks for Image Captioning. *Proc. AAAI*, 2019.
- Goyal, Y., Khot, T., Summers-Stay, D., Batra, D., and Parikh, D. Making the V in VQA matter: Elevating the role of image understanding in Visual Question Answering. In *Proc. CVPR*, 2017.
- He, K., Zhang, X., Ren, S., and Sun, J. Deep residual learning for image recognition. In *Proc. CVPR*, 2016.
- Karpathy, A. and Fei-Fei, L. Deep visual-semantic alignments for generating image descriptions. In *Proc. CVPR*, 2015.
- Kim, J.-H., On, K.-W., Kim, J., Ha, J.-W., and Zhang, B.-T. Hadamard Product for Low-rank Bilinear Pooling. In *Proc. ICLR*, 2017.
- Kim, J.-H., Jun, J., and Zhang, B.-T. Bilinear attention networks. In *Proc. NIPS*, 2018.
- Kingma, D. P. and Ba, J. Adam: A Method for Stochastic Optimization. *preprint arXiv:1412.6980*, 2014.
- Krishna, R., Zhu, Y., Groth, O., Johnson, J., Hata, K., Kravitz, J., Chen, S., Kalantidis, Y., Li, L.-J., Shamma, D. A., et al. Visual genome: Connecting language and vision using crowdsourced dense image annotations. *International Journal of Computer Vision*, 2017.
- Kulkarni, G., Premraj, V., Dhar, S., Li, S., Choi, Y., Berg, A. C., and Berg, T. L. Baby talk: Understanding and generating image descriptions. In *Proc. CVPR*, 2011.
- Lin, C.-Y. ROUGE: A package for automatic evaluation of summaries. *Text Summarization Branches Out*, 2004.
- Lin, T.-Y., Maire, M., Belongie, S., Hays, J., Perona, P., Ramanan, D., Dollár, P., and Zitnick, C. L. Microsoft coco: Common objects in context. In *Proc. ECCV*, 2014.
- Liu, F., Ren, X., Liu, Y., Wang, H., and Sun, X. simNet: Stepwise image-topic merging network for generating detailed and comprehensive image captions. In *Proc. EMNLP*, 2018a.
- Liu, X., Li, H., Shao, J., Chen, D., and Wang, X. Show, Tell and Discriminate: Image Captioning by Self-retrieval with Partially Labeled Data. In *Proc. ECCV*, 2018b.
- Lu, J., Yang, J., Batra, D., and Parikh, D. Hierarchical question-image co-attention for visual question answering. In *Proc. NIPS*, 2016.
- Lu, J., Yang, J., Batra, D., and Parikh, D. Neural baby talk. In *Proc. CVPR*, 2018.
- Malaviya, C., Ferreira, P., and Martins, A. F. Sparse and Constrained Attention for Neural Machine Translation. In *Proc. ACL*, 2018.
- Malinowski, M. and Fritz, M. A multi-world approach to question answering about real-world scenes based on uncertain input. In *Proc. NIPS*, 2014.
- Martins, A. and Astudillo, R. From Softmax to Sparsemax: A Sparse Model of Attention and Multi-Label Classification. In *Proc. ICML*, 2016.
- Nam, H., Ha, J.-W., and Kim, J. Dual attention networks for multimodal reasoning and matching. In *Proc. CVPR*, 2017.
- Niculae, V. and Blondel, M. A regularized framework for sparse and structured neural attention. In *Proc. NeurIPS*, 2017.

- Papineni, K., Roukos, S., Ward, T., and Zhu, W.-J. BLEU: a method for automatic evaluation of machine translation. In *Proc. ACL*, 2002.
- Pennington, J., Socher, R., and Manning, C. Glove: Global vectors for word representation. In *Proc. EMNLP*, 2014.
- Peters, B., Niculae, V., and Martins, A. F. Sparse Sequence-to-Sequence Models. In *Proc. ACL*, 2019.
- Ren, S., He, K., Girshick, R., and Sun, J. Faster r-cnn: Towards real-time object detection with region proposal networks. In *Proc. NIPS*, 2015.
- Russakovsky, O., Deng, J., Su, H., Krause, J., Satheesh, S., Ma, S., Huang, Z., Karpathy, A., Khosla, A., Bernstein, M., Berg, A. C., and Fei-Fei, L. ImageNet Large Scale Visual Recognition Challenge, 2014.
- Tan, H. and Bansal, M. LXMERT: Learning Cross-Modality Encoder Representations from Transformers. In *Proc. EMNLP*, 2019.
- Tao, Q., Yang, H., and Cai, J. Zero-annotation object detection with web knowledge transfer. In *Proc. ECCV*, 2018.
- Tibshirani, R., Saunders, M., Rosset, S., Zhu, J., and Knight, K. Sparsity and smoothness via the fused lasso. *Journal of the Royal Statistical Society: Series B (Statistical Methodology)*, 2005.
- Vaswani, A., Shazeer, N., Parmar, N., Uszkoreit, J., Jones, L., Gomez, A. N., Kaiser, Ł., and Polosukhin, I. Attention is all you need. In *Proc. NeurIPS*, 2017.
- Vedantam, R., Lawrence Zitnick, C., and Parikh, D. CIDEr: Consensus-based image description evaluation. In *Proc. CVPR*, 2015.
- Wang, W., Chen, Z., and Hu, H. Hierarchical Attention Network for Image Captioning. In *Proc. AAAI*, 2019.
- Xin, B., Kawahara, Y., Wang, Y., Hu, L., and Gao, W. Efficient generalized fused lasso and its applications. *ACM Trans. Intell. Syst. Technol.*, 2016.
- Xu, H. and Saenko, K. Ask, attend and answer: Exploring question-guided spatial attention for visual question answering. In *Proc. ECCV*, 2016.
- Xu, K., Ba, J., Kiros, R., Cho, K., Courville, A., Salakhudinov, R., Zemel, R., and Bengio, Y. Show, attend and tell: Neural image caption generation with visual attention. In *Proc. ICML*, 2015.
- Yang, Z., He, X., Gao, J., Deng, L., and Smola, A. Stacked attention networks for image question answering. In *Proc. CVPR*, 2016.
- Young, P., Lai, A., Hodosh, M., and Hockenmaier, J. From image descriptions to visual denotations: New similarity metrics for semantic inference over event descriptions. *Transactions of the Association for Computational Linguistics*, 2014.
- Yu, Y. On decomposing the proximal map. In *Proc. NeurIPS*, 2013.
- Yu, Z., Yu, J., Fan, J., and Tao, D. Multi-modal factorized bilinear pooling with co-attention learning for visual question answering. In *Proc. ICCV*, 2017.
- Yu, Z., Yu, J., Xiang, C., Fan, J., and Tao, D. Beyond bilinear: Generalized multimodal factorized high-order pooling for visual question answering. *IEEE transactions on neural networks and learning systems*, 2018.
- Yu, Z., Yu, J., Cui, Y., Tao, D., and Tian, Q. Deep Modular Co-Attention Networks for Visual Question Answering. In *Proc. CVPR*, 2019.

Supplementary material

A Forward and backward passes of 2D fusedmax attention.

A.1 Preliminaries

The **proximal operator** of a function $f: \mathbb{R}^d \rightarrow \mathbb{R} \cup \{\infty\}$ is defined as

$$\text{prox}_f(\mathbf{z}) = \arg \min_{\mathbf{w} \in \mathbb{R}^d} f(\mathbf{w}) + \frac{1}{2} \|\mathbf{w} - \mathbf{z}\|_2^2, \quad (12)$$

and it is guaranteed to have a unique solution, thanks to the strong convexity of the Euclidean distance.

The **indicator function** of a set $\mathcal{C} \subset \mathbb{R}^d$ is the function

$$\iota_{\mathcal{C}}: \mathbb{R}^d \rightarrow \mathbb{R} \cup \{\infty\}, \quad \iota_{\mathcal{C}}(\mathbf{w}) := \begin{cases} 0, & \mathbf{w} \in \mathcal{C}, \\ \infty, & \mathbf{w} \notin \mathcal{C}. \end{cases} \quad (13)$$

The **projection onto a convex set** $\mathcal{C} \subset \mathbb{R}^d$ is defined as

$$\text{proj}_{\mathcal{C}}(\mathbf{z}) := \arg \min_{\mathbf{w} \in \mathcal{C}} \frac{1}{2} \|\mathbf{z} - \mathbf{w}\|_2^2 = \text{prox}_{\iota_{\mathcal{C}}}(\mathbf{z}), \quad (14)$$

showing that the proximal operator can be seen as a generalization of projection.

The **sparsemax** attention mapping (Martins & Astudillo, 2016) is the projection onto the simplex,

$$\text{sparsemax}(\mathbf{z}) := \text{proj}_{\Delta}(\mathbf{z}) = \arg \min_{\mathbf{p} \in \Delta} \frac{1}{2} \|\mathbf{p} - \mathbf{z}\|_2^2. \quad (15)$$

A necessary component for using sparsemax for attention is its Jacobian, the matrix of its partial derivatives $(\mathbf{J}_{\text{sparsemax}})_{i,j} = \frac{\partial \text{sparsemax}(\mathbf{z})_i}{\partial z_j}$. Martins & Astudillo (2016) derive its expression

$$\mathbf{J}_{\text{sparsemax}}(\mathbf{z}) = \text{diag } \mathbf{s} - \frac{1}{\|\mathbf{s}\|_1} \mathbf{s} \mathbf{s}^\top, \quad (16)$$

where $s_j = 1$ if $\text{sparsemax}(\mathbf{z})_j > 0$ and $s_j = 0$ otherwise.

A.2 Proof of Proposition 1

Proof. This result is a slight extension of Proposition 2 in Niculae & Blondel (2017), and also follows from Corollary 4 of Yu (2013), by taking $f = \iota_{\Delta}$, and noting that ι_{Δ} is symmetric: if $\mathbf{p} \in \Delta$, then any vector \mathbf{p}' obtained by permuting \mathbf{p} is also in Δ , because its values remain non-negative and sum to 1. \square

A.3 Proof of Proposition 2

Let $\mathbf{w}^* := \text{prox}_{\lambda \Omega_E}$, and denote by G_i the set of indices fused to w_i in the solution. Define $s_{ij} = \text{sign}(w_i^* - w_j^*)$.

Proof. The subgradient optimality conditions of Eq. 4 are: (Friedman et al.)

$$w_i^* - z_i + \sum_{k:i \sim k} \lambda t_{ik} - \sum_{k:k \sim i} \lambda t_{ki} = 0, \quad 1 \leq i \leq d. \quad (17)$$

where $t_{ij} = \text{sign}(w_i^* - w_j^*)$ if $w_i^* \neq w_j^*$, otherwise t_{ij} is a free variable in $[-1, 1]$.

We focus on a single group $G = G_i$, dropping the index i for brevity. Within a fused group, the solution is constant, i.e., $w_j^* = w$ for $j \in G$. We separate the sums in Eq. 17 according to whether $k \in G$ or not, and move the ‘‘constant’’ terms to the right hand side, yielding the system

$$w + \sum_{\substack{j \sim k \\ k \in G}} \lambda t_{jk} - \sum_{\substack{k \sim j \\ k \in G}} \lambda t_{kj} = z_j + \sum_{\substack{k \sim j \\ k \notin G}} \lambda s_{kj} - \sum_{\substack{j \sim k \\ k \notin G}} \lambda s_{jk}, \quad j \in G. \quad (18)$$

Summing up the Eq. 18 over all $j \in G$, we observe that for any $k \in G$, the term $\lambda_{t_{jk}}$ appears twice with opposite signs. Thus,

$$\sum_{j \in G} w = \sum_{j \in G} \left(z_j + \sum_{\substack{k \sim j \\ k \notin G}} \lambda_{s_{kj}} - \sum_{\substack{j \sim k \\ k \notin G}} \lambda_{s_{jk}} \right). \quad (19)$$

Dividing by $|G|$ gives exactly Eq. 10. This reasoning applies to any group G_i . □

B Examples

The complete sequence of attention maps corresponding to the caption generation of the example in Figure 1 is presented in Figure 3 and another example is presented in Figure 4. An additional example of VQA is presented in Figure 5

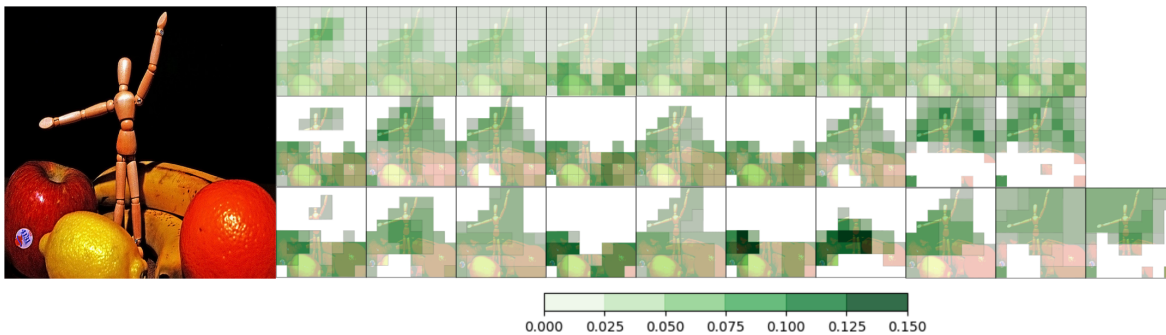


Figure 3: Example generated captions using softmax attention (top), sparsemax attention (middle) and TVMAX attention (bottom). The captions are “A bowl of fruit and a bowl of fruit”, “A bowl of fruit and oranges on a table” and “A bowl of oranges and a banana on a table”.

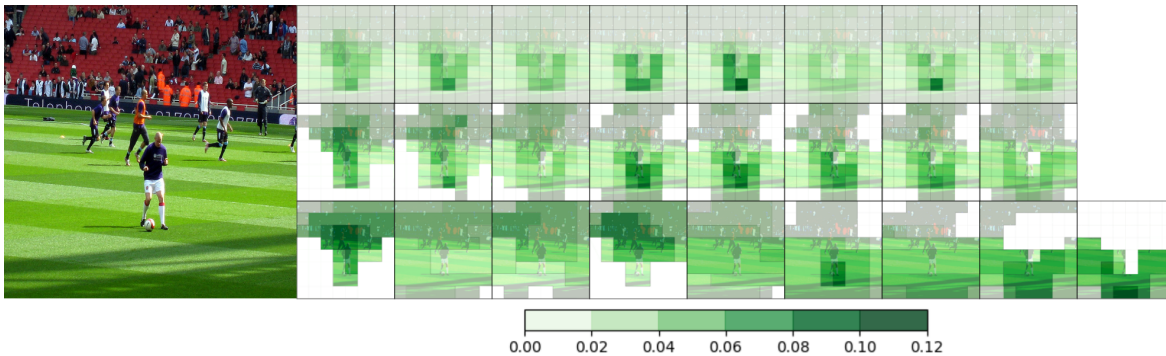


Figure 4: Example generated captions using softmax attention (top), sparsemax attention (middle) and TVMAX attention (bottom). The captions are “A soccer player is running to the base”, “A soccer player is running to the field” and “A group of people playing soccer on a field”.

C Human evaluation description

To perform the human evaluation firstly 100 images were randomly selected from the test set of the MSCOCO dataset (using the split proposed by Karpathy & Fei-Fei (2015)). For each of the selected images, the human evaluators selected a score from 1 to 5 for the captions generated by the models using softmax attention, sparsemax attention, and TVMAX attention. They were also asked to evaluate whether the models attend to the relevant regions of the image when generating a certain word. For that they observed the attention plots corresponding to the non stop words of the caption of each of the models. While in Figures 1, 3, and 4 we emphasized sparsity with

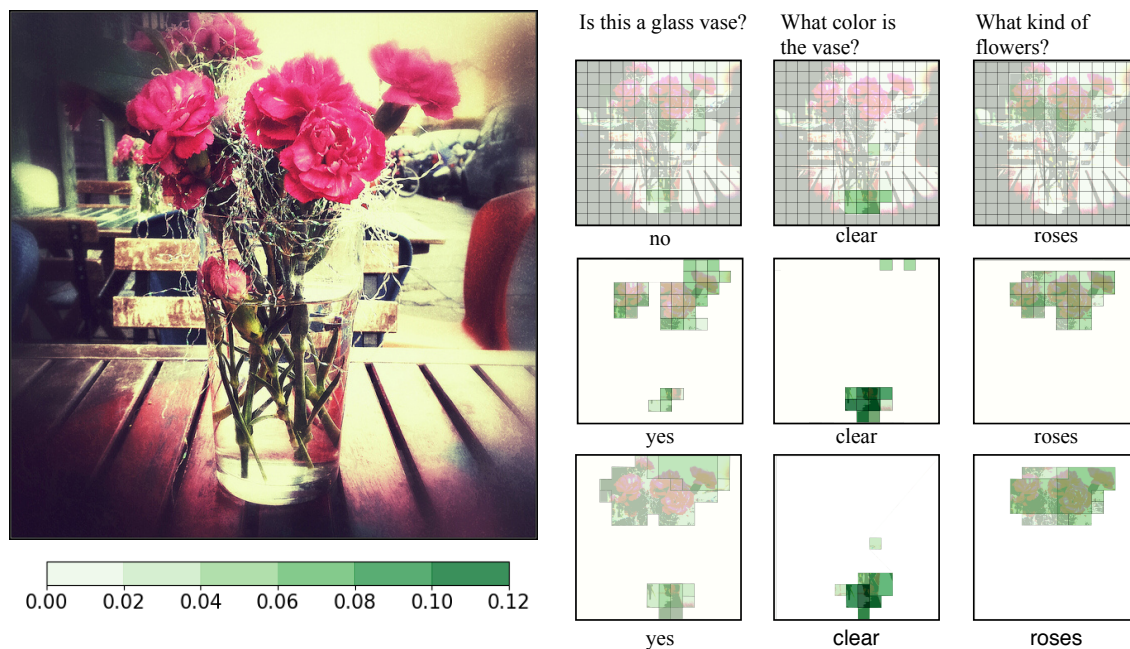


Figure 5: VQA using softmax (top), sparsemax (middle) and TVMAX attention (bottom). Shading denotes the attention weight, with white for zero attention.

a hard white mask, for the human evaluation the sparse regions of the attention plots were simply fully transparent, to avoid biasing the evaluators. The possible scores were also between 1 and 5. The 100 images were judged by 6 persons both for the captions evaluation and attention evaluation. The order of the captions and attention plots was randomly chosen for each image.

With these scores, we computed the mean of the captions evaluation scores and the mean of the attention relevance evaluation scores. The results are reported in Table 2.